Journal of
Experimental
Botany
www.jxb.oxfordjournals.org

RESEARCH PAPER

Two alanine aminotranferases link mitochondrial glycolate oxidation to the major photorespiratory pathway in *Arabidopsis* and rice

Markus Niessen[1], Katrin Krause[1], Ina Horst[1], Norma Staebler[2,*], Stephanie Klaus[2,†], Stefanie Gaertner[2,‡], Rashad Kebeish[1,§], Wagner L. Araujo[3], Alisdair R. Fernie[3] and Christoph Peterhansel[1,¶]

[1] Leibniz University Hannover, Institute of Botany, D-30419 Hannover, Germany
[2] RWTH Aachen, Institute of Botany, D-522056 Aachen, Germany
[3] Max Planck Institute of Molecular Plant Physiology, D-14476 Potsdam-Golm, Germany

* Present address: Institute of Biotechnology I, Forschungszentrum Juelich, Juelich, Germany.
† Present address: Spintec Engineering GmbH, D-52066 Aachen, Germany
‡ Present address: Institute of Biology I, RWTH Aachen, D-52056 Aachen, Germany
§ Present address: Botany Department, Faculty of Science, Zagazig University, Egypt
¶ To whom correspondence should be addressed. E-mail: cp@botanik.uni-hannover.de

Abstract

The major photorespiratory pathway in higher plants is distributed over chloroplasts, mitochondria, and peroxisomes. In this pathway, glycolate oxidation takes place in peroxisomes. It was previously suggested that a mitochondrial glycolate dehydrogenase (GlcDH) that was conserved from green algae lacking leaf-type peroxisomes contributes to photorespiration in *Arabidopsis thaliana*. Here, the identification of two *Arabidopsis* mitochondrial alanine:glyoxylate aminotransferases (ALAATs) that link glycolate oxidation to glycine formation are described. By this reaction, the mitochondrial side pathway produces glycine from glyoxylate that can be used in the glycine decarboxylase (GCD) reaction of the major pathway. RNA interference (RNAi) suppression of mitochondrial ALAAT did not result in major changes in metabolite pools under standard conditions or enhanced photorespiratroy flux, respectively. However, RNAi lines showed reduced photorespiratory CO_2 release and a lower CO_2 compensation point. Mitochondria isolated from RNAi lines are incapable of converting glycolate to CO_2, whereas simultaneous overexpression of GlcDH and ALAATs in transiently transformed tobacco leaves enhances glycolate conversion. Furthermore, analyses of rice mitochondria suggest that the side pathway for glycolate oxidation and glycine formation is conserved in monocotyledoneous plants. It is concluded that the photorespiratory pathway from green algae has been functionally conserved in higher plants.

Key words: Aminotransferase, mitochondrion, photorespiration, plant evolution.

Introduction

Under moderate growth conditions, ribulose-1,5-bisphosphate carboxylase/oxygenase (Rubisco) fixes molecular oxygen (O_2) instead of carbon dioxide (CO_2) in approximately one out of four reactions which results in the formation of phosphoglycolate (Sharkey, 1988). Photorespiration is the only plant pathway for the further conversion of this abundant reaction product (reviewed in Peterhansel *et al.*, 2010). After

dephosphorylation, glycolate is exported from the chloroplast and oxidized to glyoxylate by glycolate oxidase in the peroxisome. O_2 is the electron acceptor during this reaction and H_2O_2 is formed that is detoxified by catalase. Still in the peroxisome, glyoxylate is transaminated to glycine by glutamate:glyoxylate aminotransferases. Glycine is transported to the mitochondrion where two molecules of glycine

form one molecule of serine that is transported back to the peroxisome. This reaction is catalysed by the glycine decarboxylase complex. CO_2 and NH_3 are released during this reaction. These losses are the major reason why photorespiration is often viewed as a wasteful biochemical process (Maurino and Peterhansel, 2010). Serine is deaminated to hydroxypyruvate by serine:glyoxylate aminotransferase and the amino group is used for the simultaneous amination of glyoxylate to glycine. Hydroxypyruvate is further converted to glycerate in the peroxisome. Glycerate is transported back to the chloroplast and phosphorylated to phosphoglycerate which can be integrated into the Calvin cycle. By this complex series of reactions, up to three-quarters of the carbon in phosphoglycolate is rescued and made available for plant metabolism.

Leaf-type peroxisomes containing glycolate oxidase are an invention of charophytes, multicellular green algae that are the direct ancestors of land plants (Raven, 2000). Chlorophytes, the second major lineage of green algae, do not possess such peroxisomes. Photorespiratory metabolism is mainly confined to the mitochondrion in this clade. Nevertheless, the main reaction steps, including oxidation of glycolate, transamination, decarboxylation, and serine formation, as well as recycling of phosphoglycerate, are probably identical (Stabenau and Winkler, 2005). For glycolate oxidation, chlorophytes make use of a glycolate dehydrogenase (GlcDH) that uses organic co-substrates instead of O_2 (Paul and Volcani, 1976). Characterization of a knock-out strain for the gene encoding GlcDH in *Chlamydomonas* revealed that photorespiration is essential for chlorophyte growth (Nakamura *et al.*, 2005) despite the effective carbon-concentrating mechanism expressed by these algae (Spalding, 2008). The enzymes catalysing the further reactions of mitochondrial photorespiration in *Chlamydomonas* have not been isolated to date.

Previous analyses suggested that the chlorophyte GlcDH has been conserved in higher plants. A homologous enzyme (encoded by At5g06580) is targeted to the mitochondria, can oxidize glycolate, and uses D-lactate as an alternative substrate. The latter is a common feature of GlcDH enzymes that discriminates this enzymatic activity from glycolate oxidases (Bari *et al.*, 2004). Furthermore, an *Arabidopsis* T-DNA insertion line that does not express GlcDH showed reduced photorespiratory flux as estimated from gas exchange measurements and metabolite concentrations under low CO_2 conditions (Niessen *et al.*, 2007). However, the mutant showed no obvious phenotype under normal growth conditions (Niessen *et al.*, 2007). These data suggested that the chlorophyte photorespiratory pathway including the mitochondrial glycolate oxidation step was conserved in *Arabidopsis*, but that peroxisomal reactions of the major pathway evolved in addition. This view was recently challenged by characterization of the enzymatic properties of the recombinant purified enzyme *in vitro*. The catalytic efficiency of the recombinant enzyme with D-lactate as a substrate was much higher than with glycolate, and the mutant survived growth on high glycolate, but not D-lactate concentrations (Engqvist *et al.*, 2009). These data imply that the main function of

GlcDH in higher plants might be conversion of D-lactate, an intermediate of methylglyoxal detoxification (Rasmusson *et al.*, 2008).

Here two mitochondrial aminotransferases from *Arabidopsis* are identified that link mitochondrial glyoxylate production from glycolate to the formation of glycine and, thus, to the major photorespiratory pathway. The same enzymatic reactions can also be identified in rice mitochondria. These results define the components of a mitochondrial glycolate oxidation pathway in higher plants.

Materials and methods

Plant material and growth conditions

Arabidopsis thaliana wild-type plants and mutants (ecotype Col-0) were grown under short-day conditions (8 h illumination and 16 h darkness) in growth chambers at 22 °C with a light intensity of 100 μmol m^{-2} s^{-1}. T-DNA insertion mutants were ordered from the Nottingham Arabidopsis Stock Centre (NASC). Homozygous mutants were identified by PCR using the primers and conditions as suggested by NASC. For metabolite analysis, plants were grown for 5–6 weeks under standard conditions (8 h illumination and 16 h darkness with 400 ppm CO_2). Half of the plants were shifted 24 h before harvesting to 100 ppm CO_2. *Oryza sativa* (cultivar Guarà) and *Nicotiana tabacum* (cultivar Petite Havana) were grown in a greenhouse with supplemental illumination under semi-controlled conditions. The daily light rhythm was 16 h light and 8 h of darkness. In addition to sunlight, lamps ensured a minimum light intensity of at least 250 μmol m^{-2} s^{-1}.

Cloning and recombinant protein expression of ALAAT2

*Alaat*2 was amplified by PCR using *Arabidopsis* leaf cDNA as a template and gene-specific primers (5′-GGCGATGGCCAATGCG-GAGATTCTTGATTAACC-3′ and 5′-CGGAACTCGAGGTTG-CGGAACTCGTCCATGAA-3′). The primers contain extensions with *Msc*I and *Xho*I restriction sites. PCR fragments were cut and ligated into the plasmid pET22b(+) (Novagen, Darmstadt, Germany). Recombinant protein was expressed as described in Bari *et al.* (2004). For bacterial lysis, the bacterial pellet was resuspended in lysis buffer (20 mM TRIS-HCl pH 7.6, 10% glycerol, 0.1% Triton X-100, 0.5% lysozyme, 5 mM dithiothreitol (DTT), and 1× Complete protease inhibitor (Roche, Mannheim, Germany) and incubated for 1 h on ice. The suspension was centrifuged twice at 36 000 *g* for 10 min at 4 °C. The supernatant was used for the assays.

Cloning of red fluorescent protein (RFP) constructs

*Alaat*1 and *Alaat*2 full-length sequences were amplified by PCR using *Arabidopsis* leaf cDNA as a template and gene-specific primer combinations (5′-ACATCCATGGTAT-GCGGAGATTCGTGATTGGCCAA-3′ and 5′-TGCTCC-ATGGTGTCGCGGAACTCGTCCATGGA-3′ for *Alaat*1, and 5′-AGCCGTCTCCCATGGTATGCGGAGATTC-3′ and 5′-TGCATGGGAGACGCTCGAGGTTGCGGAA-3′ for *Alaat*2). The amplified constructs were cloned into the binary plant expression vector pTRAK, a derivative of pPAM (GenBank accession no. AY027531), in translational fusion to a modified dsRED protein (Jach *et al.*, 2001).

Generation of RNAi lines

For down-regulation of *Alaat*1 and *Alaat*2 expression by RNA interference (RNAi), stem–loop constructs containing homologous sequences were used. The *Alaat*1 RNAi construct contains the

sequence corresponding to position 1821–2020 of the full-length cDNA. The *Alaat*1 and *Alaat*2 double RNAi construct contains the sequence corresponding to position 1252–1451 of the full-length *Alaat*1 cDNA. PCR products were cloned into pJawohl8-RNAi vector (GenBank accession no. AF408413; kindly provided by I.E. Somssich MPI for Plant Breeding Research, Cologne) using the Gateway® technology (Invitrogen, Leck, The Netherlands). Resulting constructs were transferred into *Agrobacterium tumefaciens* GV3101 and used for plant transformation. *Arabidopsis thaliana* Col-0 wild-type plants were transformed using the floral dip method (Clough and Bent, 1998). Gene expression in knock-down lines was measured by quantitative reverse transcription-PCR (RT-PCR).

Transient overexpression in Nicotiana tabacum

Transient transformation was carried out on intact tobacco plants. *Agrobacterium tumefaciens* strain GV3101 (pMP90RK, Gm^R Km^R Rif^R) was transformed with plant expression vectors containing *Alaat*1 and *GlcDH* coding sequences. *Alaat*1 and *GlcDH* full-length coding sequences were amplified by PCR using *Arabidopsis* leaf cDNA as a template. The amplified constructs were cloned into the binary plant expression vector pTRAK, a derivative of pPAM (GenBank accession no. AY027531). Transformation was carried out as described in Sparkes *et al.* (2006) with minor modifications. Plants used for transformation were 6–7 weeks old and were grown in the greenhouse. Plants were infiltrated with agrobacteria resuspended in infiltration medium [8.86 g l^{-1} MS (Murashige and Skoog) medium, 100 g l^{-1} sucrose, 20 mM MES, and 0.2 mM acetosyringone] and kept for 2 d in a phytochamber with a daily rhythm of 16 h light and 8 h darkness.

Quantitative RT-PCR

RNA was prepared from *Arabidopsis* leaves following the 1-bromo-3-chlorpropane method (Chomczynski and Mackey, 1995). The integrity of the preparation was tested by gel electrophoresis. One unit of DNase I (MBI Fermentas, St Leon-Rot, Germany) per microgram of RNA and 1× DNase buffer were added and the reactions were incubated for 30 min at 37 °C, followed by a denaturation step of 15 min at 70 °C to remove traces of contaminating DNA. Approximately 1 μg of RNA was mixed with 50 pmol random nonamer primer, heated for 5 min to 70 °C, and cooled down on ice before adding 200 U of MMLV reverse transcriptase (Promega, Mannheim, Germany) and 1 mM dNTPs in reaction buffer supplied by the manufacturer. Samples were incubated for 60 min at 37 °C and reverse transcriptase was inactivated at 70 °C for 10 min. Quantitative RT-PCR was performed on an ABI PRISM 7300 (Applied Biosystems, Darmstadt, Germany) using SYBR Green fluorescence (Platinum SYBR Green qPCR Mix (Invitrogen) for detection. Primer combinations were 5′-GGTAACATTGTGCTCAGTGGT-GG-3′ and 5′-GGTGCAACGACCTTAATCTTCAT-3′ for *Actin*2, 5′-GGAGCTATGTATCTATTCCCTTGCC-3′ and 5′-TTAAGAATTCGTTTGCAGTAGAAATTG-3′ for *Alaat*1, 5′-GGAGCAATGTATCTCTTCCCGCGAA-3′ and 5′-GAAGAATTCGTTTGCAGTAGAACGCA-3′ for *Alaat*2, 5′-CCG TTA CCT CAG ATG CTT GAT TC-3′ and 5′-CTC TGA AGA GCT AAT TCC CAT TAT G-3′ for At5g44800, 5′-GGT TGA TGC TCA TGT TAA AGC TCT TC-3′ and 5′-GCG TAA TCA CCT GCA CGT CTA G-3′ for At1g30620, 5′-CGA GCG GAT TCG AAC TAG TTG G-3′ and 5′-CTG GCC AAG TAT ATC CGC TAC TG-3′ for At1g52220, 5′-CGA ATC AAC CCT TCT CGA GCA C-3′ and 5′-CTC TTC TTT GCT GCA CTC TCT GC-3′ for At3g16170, 5′-CAT CGG ACC TGA CAC TGT ATC-3′ and 5′-CTG ACA CAT TCG CAT CTA TTG TC-3′ for At5g13420, 5′-GTT CTC GAA TAT TTG GCC GCC G-3′ and 5′-GCT TAG CTC CTC ATC GTT TCT G-3′ for At5g54640, 5′-CAG TTC TCA CAT CAA TTC AGT CTT TG-3′ and 5′-CTG AAC AAC CTT GCA GCC TCT G-3′ for At5g62540, 5′-CAT TGT GCT GAA GTT GGT TCA C-3′ and 5′-CGG TCA CTC

ACA AGC TCA ATC-3′ for At4g39660, 5′-GAA TGG ATA AGT AAC ACA GTG AC-3′ and 5′-CAT TTC CTA GGT GTC CAA TTC TG-3′ for At2g13360, 5′-GTG GAG CTG GTG AGT GAT CGC-3′ and 5′-TGA AGC AGA GAG GTG GTG TGA TTC-3′ for At2g38400, 5′-CAC AGA AGG TGC TAT GTA TTC ATT C-3′ and 5′-GAG ATT CCT GTG GCT TCT AAG AG-3′ for At1g70580, 5′-CTC ATG ACA GAT GGA TTC AAC AG-3′ and 5′-GGA GAG CTC CCG TTG GTA AC-3′ for At1g23310, and 5′-CAT TGG AGA CGT GAG AGG GAG-3′ and 5′-CAT TCC CAT AGA ATC ACC CTT TCC-3′ for At3g08860.

Subcellular localization

For dsRED localization and mitochondrial staining, leaves were collected from 4-week old plants and cut into small pieces. Protoplasts were isolated by incubating the leaf pieces in protoplast isolation buffer [0.5 M sorbitol, 5 mM MES pH 5.8, 10 mM $CaCl_2$, 3% (v/v) Rohament CL, 2% (v/v) Rohament PL, and 0.12% (w/v) Mazeroenzyme] at 30 °C for 2 h under illumination. The solution was filtered through a 100 μm sieve and the flowthrough was carefully collected. The protoplast suspension was diluted with 0.5 vol. of Linsmeier/Skoog medium (0.36% MS and 0.27 M NaCl pH 5.8) and centrifuged for 5 min at 500 *g*. The protoplast pellet was carefully resuspended in Linsmeier/Skoog medium. Part of the protoplasts was stained with MitoTracker®GreenFM (Invitrogen) as described by the supplier. Images were acquired with a ×63 oil immersion PLAN-APO objective. The entire sample was excited with 488 nm and 568 nm laser light. The confocal sections were collected using a 515–535 nm emission setting for MitoTracker®-GreenFM, 570–610 nm emission setting for dsRED, and 660–720 nm emission setting for chlorophyll fluorescence.

Gas exchange measurements

Gas exchange measurements were performed with the LI-6400 system (Li-Cor, Lincoln, NE, USA) and parameters were calculated using the software supplied by the manufacturer. Conditions were: photon flux density (PFD), 1000 μmol m^{-2} s^{-1}; chamber temperature, 26 °C, flow rate, 100 μmol s^{-1}, relative humidity, 60–70%. The post-illumination CO_2 burst was measured as described earlier (Atkin *et al.*, 1998; Niessen *et al.*, 2007). The apparent CO_2 compensation point (Γ) was deduced from A/c_i [apparent CO_2 assimilation (A)/intercellular CO_2 concentration (c_i)] curves by regression analysis in the linear range of the curve.

Isolation of mitochondria

Intact mitochondria were isolated from 4 to 6-week-old *Arabidopsis* plants. Approximately 5 g of leaves were ground in grinding buffer [50 mM HEPES-KOH pH 7.5, 1 mM $MgCl_2$, 1 mM EDTA, 1 g l^{-1} bovine serum albumin (BSA), 0.2 g l^{-1} sodium ascorbate, 0.3 M mannitol, 5 g l^{-1} polyvinylpyrrolidone (PVP)]. After filtration through three layers of Miracloth, the solution was centrifuged at 1100 *g* for 20 min. The supernatant was centrifuged again at 14 000 *g* for 30 min. The pellets were resuspended in mannitol wash buffer (10 mM HEPES-KOH pH 7.5, 0.3 M mannitol, and 1 g l^{-1} BSA). The solution was loaded on a self-forming 8 ml 45% Percoll gradient [45% Percoll, 50% sucrose-buffer (0.3 M sucrose, 10 mM HEPES-KOH pH 7.5, and 1 g l^{-1} BSA)] and centrifuged for 45 min at 40 000 *g*. The mitochondrial fraction was collected, washed in mannitol wash buffer, and resuspended in 50 mM HEPES-NaOH pH 7.5, 2 mM EDTA, 5 mM $MgCl_2$, 0.1% Triton X-100. Peroxisomal contamination in the preparation was determined by the catalase activity assay. The mitochondrial suspension was adjusted to 30 mM phosphate buffer pH 7.0, 10 mM H_2O_2, and the enzymatic activity was measured at 240 nm wavelength. According to this assay, mitochondrial fractions always showed a purity of >94%.

CO₂ release studies

[1,2-¹⁴C]Glycolate or [1-¹⁴C]glycine (Hartmann Analytics, Braunschweig, Germany), respectively, were added to a mitochondrial suspension corresponding to 50 µg of mitochondrial protein or an equivalent amount of the chloroplast/peroxisome protein fraction. Specific radioactivities were 1850 MBq mmol⁻¹ and final concentrations were 0.1 mM for both substrates. Released CO_2 was absorbed in 0.5 M NaOH. Samples were incubated overnight and NaOH was constantly mixed to absorb all released CO_2. For inhibition experiments, 1 mM aminooxyacetate (AOA) or 1 mM KCN was added to the reaction mix.

Enzymatic assays

GlcDH activity was assayed according to Lord (1972). Protein extracts were added to 10 mM potassium phosphate (pH 8.0), 0.025 mM 2,6-dichlorophenol indophenol (DCIP), 0.1 ml of 1% (w/v) phenozine methosulphate (PMS), and 10 mM potassium glycolate. At fixed time points, individual assays were terminated by the addition of 40 µl of 12 M HCl. After incubation for 10 min, 240 µl of 0.1 M phenylhydrazine was added. The mixture was incubated at room temperature for 10 min. The extinction due to the formation of glyoxylate phenylhydrazone was measured at 324 nm. Alanine:glyoxylate aminotransferase (AGA), alanine:-keto-glutarate aminotransferase (AKA), glutamate:glyoxylate aminotransferase (GGA), and glutamate:pyruvate aminotransferase (GPA) activities were measured as described before (Liepman and Olsen, 2003; Miyashita *et al.*, 2007).

Metabolite analysis

For metabolite extraction, complete shoots of plants were harvested in reaction tubes filled with liquid nitrogen to avoid any turnover of metabolites. A 50 mg aliquot of homogenized leaf material was added to 1 ml of pre-chilled extraction mix (1 vol. of H_2O, 1 vol. of $ChCl_3$, and 2.5 vols of methanol). Samples were mixed for 5 min at 4 °C. After centrifugation (16 000 *g*, 4° C, 2 min), 500 µl of the supernatant were mixed with 250 µl of H_2O and again centrifuged for 2 min. A 250 µl aliquot of the top layer (polar phase) was dried in a speed-vac concentrator. Derivatization, addition of standards, and sample injection were performed as described in Lisec *et al.* (2006). Chromatograms and mass spectra were analysed and evaluated using TAGFINDER (Luedemann *et al.*, 2008) and ChromaTOF® (LECO Corporation) software. The highest peak area in a data set was arbitrarily set to 1000 and all other peak areas were calculated relative to this number.

Statistics

Significance was determined according to two-sided homoscedastic *t*-test using Excel software (Microsoft, Munich, Germany).

Results

Glycolate to CO_2 conversion was compared in isolated *Arabidopsis* mitochondria in the presence and absence of the aminotransferase inhibitor AOA in order to test whether an aminotransferase is involved in this process. [¹⁴C]Glycolate was added to isolated mitochondria and the released radioactive ¹⁴CO_2 was captured in NaOH solution as described before (Niessen *et al.*, 2007). As shown in Fig. 1, the amount of CO_2 liberated from glycolate was strongly reduced in the presence of AOA compared with the control. The inhibition by AOA of ¹⁴CO_2 release from [¹⁴C]glycine was also tested, because glycine decarboxylase (GDC) has been reported to be inhibited by high AOA concentrations (Sarojini and Oliver, 1985). Only a slight reduction in CO_2 release from
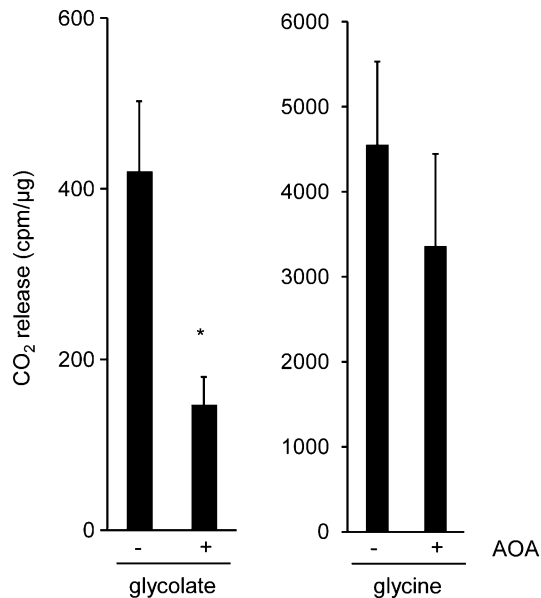

Fig. 1. Inhibition of mitochondrial glycolate metabolism by aminooxyacetate (AOA). Isolated *Arabidopsis* mitochondria corresponding to 50 µg of protein were incubated with [¹⁴C]glycolate or [¹⁴C]glycine. AOA (1 mM) was added as inhibitor. ¹⁴CO_2 released was captured in NaOH and determined by scintillation counting. Shown are the means ±SE from three independent experiments. cpm, counts per minute; *$P < 0.05$.

glycine was observed in this assay, indicating that GDC activity was not significantly affected by the assay conditions.

Mitochondrial extracts were next tested for aminotransferase activities using different amino donor and amino acceptor substrates (Fig. 2). Substrates were selected based on previous experiments with photorespiratory aminotransferases (Liepman and Olsen, 2003); however, it was not possible to measure serine:glyoxylate aminotransferase (SGAT) activity due to unavailability of hydroxypyruvate reductase that is necessary for coupling of serine deamination to NADH consumption. A fraction from a density gradient purification containing chloroplasts and peroxisomes was used for comparison. As shown in Fig. 2, most tested aminotransferase activities were almost exclusively associated with the chloroplast and peroxisome fraction. However, AGA activity was evenly distributed over the tested fractions.

The *Arabidopsis* genome contains eight sequences for putative alanine aminotransferases (Liepman and Olsen, 2003; see Table 1). Candidates were selected from these sequences by analysing coding sequences. Each of the proteins shows homology to one out of three unrelated alanine aminotransferases from mammals, respectively. AGT1 has been shown before to encode the peroxisomal SGAT (Liepman and Olsen, 2001), whereas GGT1 and GGT2 encode peroxisomal glutamate:glyoxylate aminotransferases (GGATs; Igarashi *et al.*, 2003; Liepman and Olsen, 2003). Little is known about the function of AGT2, AGT3, and PYD4, but all these enzymes show both N-terminal targeting sequences for mitochondria and/or chloroplasts and in addition C-terminal targeting sites for peroxisomes. For

AGT2, dual targeting has been experimentally verified (Carrie *et al.*, 2009). ALAAT1 [identical to AOAT4 in Igarashi *et al.* (2003) and AtAlaATc in Liepman and Olsen (2003)] and ALAAT2 [identical to AOAT3 in Igarashi *et al.* (2003) and AtAlaATm in Liepman and Olsen (2003)] belong to the same class as GGT1 and GGT2, but form a subclade and are most probably localized in mitochondria based on prediction software and proteome analyses (Lee *et al.*, 2008). No peroxisomal targeting sequence is present
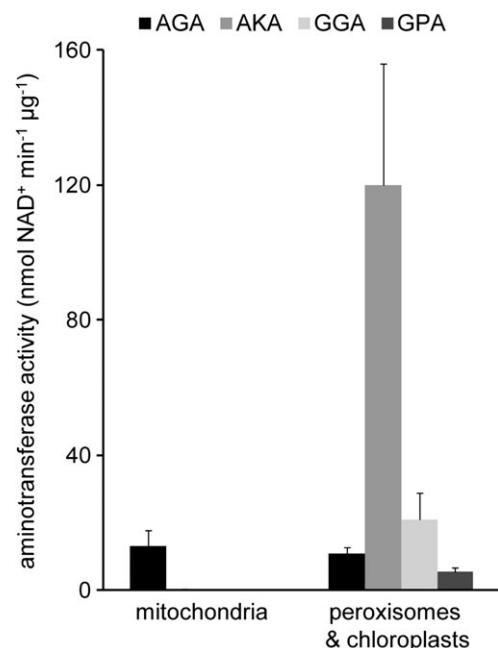

Fig. 2. Measurement of endogenous aminotransferase activity with different amino donor and acceptor substrates. Activities were measured from isolated mitochondria in comparison with a fraction from density gradient purification containing chloroplasts and peroxisomes. Shown are the means ±SE from four independent experiments. AGA, alanine:glyoxylate aminotransferase activity; AKA, alanine:keto-glutarate aminotransferase activity; GGA, gluta-mate:glyoxylate aminotransferase activity; GPA, glutamate:pyruvate aminotransferase activity.

at the C-terminus of these proteins. Targeting of both enzymes to mitochondria was verified by C-terminal fusion to RFP. As shown in Fig. 3, the red fluorescence (Fig. 3F, I) co-localizes with the MitoTracker stain that labels mito-chondria in all cases (Fig. 3B, E, H), indicating that the proteins were targeted to mitochondria *in vivo*. ALAAT1 and ALAAT2 share extremely high amino acid homology (85% identity and 93% similarity). According to Genevesti-gator (Hruz *et al.*, 2008), both genes show little regulation on the mRNA level with respect to developmental or en-vironmental stimuli. The genes are significantly expressed in all tested tissues, with the highest expression in pollen. There is no evident co-regulation with photorespiratory enzymes or *Arabidopsis* GlcDH.

Recombinant ALAAT2 was overexpressed in *Escherichia coli* and aminotransferase activity was tested with different substrates. As shown in Fig. 4, the recombinant enzyme showed the highest AGA activity, but other tested substrate combinations were used with similar efficiency. This is typical for alanine aminotransferases that use multiple substrates with similar efficiencies in *in vitro* assays (Liepman and Olsen, 2003).

Using a stem–loop construct with homologous sequences, expression of *Alaat*1 and *Alaat*2 was down-regulated in *Arabidopsis* by RNAi. The two individual mRNAs as well as a sequence region that was shared by *Alaat*1 and *Alaat*2 transcripts were targeted. The generation of efficient RNAi lines for *Alaat*2 was not successful for unknown reasons. However, *Alaat*1 mRNA levels were reduced to <25% of the wild-type control in RNAi 1 plants (Fig. 5). Both *Alaat*1 and *Alaat*2 were suppressed to similar levels in the RNAi 1/2 plants (Fig. 5). An aim was to use the available T-DNA insertion lines (NASC codes N583084, N504925, N607662, and N655815), but significant accumulation of *Alaat* mRNA was detectable in all these lines (data not shown). As RNAi suppression was partially lost in successive generations, T_1 plants with independent transgene integration sites were exclusively used for all experiments. Before starting physio-logical analyses, reduction of *Alaat*1 and *Alaat*2 mRNA levels was always tested for each individual plant. To exclude

Table 1. Putative alanine aminotransferases in the *Arabidopsis* genome

TAIR gene symbol	AGI code	Nearest human homologue[a]	Aminotransferase class[b]	Localization (evidence[c])	Source
AGT1	At2g13360	HsAGT1 (gi178273)	V	Peroxisomal (E)	Liepman and Olsen (2001); Reumann *et al.* (2009)
AGT2	At4g39660	HsAGT2 (gi54312043)	III	Mito./perox. (E)	Carrie *et al.* (2009)
AGT3	At2g38400			Mito./perox./chloroplast (P)	SUBA II; Heazlewood *et al.* (2007)
PYD4	At3g08860			Mito/perox. (P)	SUBA II; Heazlewood *et al.* (2007)
GGT1	At1g23310	HsAlaAT1 (gi4885351)	I/II	Peroxisomal (E)	Igarashi *et al.* (2003)
GGT2	At1g70580			Peroxisomal (E)	Reumann *et al.* (2009)
ALAAT1	At1g17290			Mitochondrial (E), cytoplasmic (E)	Lee *et al.* (2008); Igarashi *et al.* (2003)
ALAAT2	At1g72330			Mitochondrial (P)	TargetP; Emanuelsson *et al.* (2000)

[a] According to BLAST (http://blast.ncbi.nlm.nih.gov).
[b] According to PFAM search (http://pfam.janelia.org/).
[c] E, experimental; P, prediction.

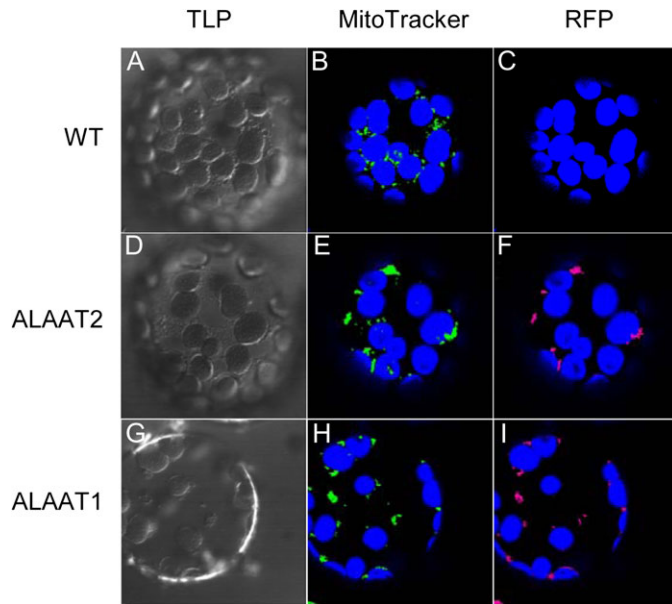|	TLP	MitoTracker	RFP
WT	A	B	C
ALAAT2	D	E	F
ALAAT1	G	H	I

Fig. 3. Subcellular localization of ALAAT1 and ALAAT2. Protoplasts were isolated from wild-type plants (A–C), plants overexpressing the ALAAT2–RFP fusion construct (D–F), and plants overexpressing the ALAAT1–RFP fusion construct (G–I). A, D, and G show transmitted light pictures (TLP) of the isolated protoplasts. B, E, and H show chlorophyll fluorescence (blue) and fluorescence of the Mito-Tracker® (green). C, F, and I show chlorophyll fluorescence in addition to RFP fluorescence (magenta). Images were acquired with a ×63 oil immersion PLAN-APO objective. The entire sample was excited with 488 nm and 568 nm laser light. The confocal sections were collected using a 515–535 nm emission setting for Mito-Tracker®GreenFM, 570–610 nm emission setting for RFP, and 660–720 nm emission setting for chlorophyll fluorescence.

that additional homologous mRNAs were affected by expression of the RNAi construct, accumulation of the seven mRNAs with highest homology to the targeted sequence region and of all mRNAs encoding putative ALAATs was also measured (Table 1). All control mRNAs accumulated to similar levels in wild-type, RNAi 1, and RNAi 1/2 leaves (Supplementary Fig. S1 available at *JXB* online).

To confirm down-regulation of ALAAT1 and ALAAT2 on the protein level, enzymatic activities from leaf extracts of the different genotypes were measured (Fig. 6). All experiments were performed in the presence and absence of AOA to discriminate between aminotransferase activity and any other enzymatic conversion. Using alanine and glyoxylate as substrates (Fig. 6A), a significant reduction in activity was detectable in both RNAi lines. However, in both single and double knock-downs, activities were still ~70% of wild-type levels. To investigate whether remaining activity levels are due to the presence of other aminotransferases such as peroxisomal GGT1 that also shows high activity with alanine and glyoxylate as substrates (Igarashi *et al.*, 2003), aminotransferase activity was additionally measured with alanine and ketoglutarate as substrates (Fig. 6B). In this assay, activities were reduced to <40% in the RNA 1/2 line compared with the wild type. In the RNAi
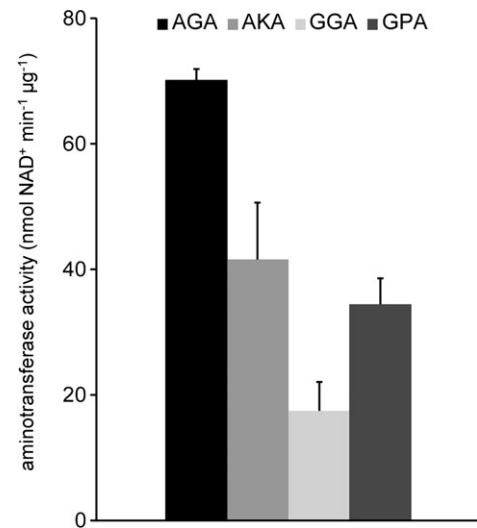

Fig. 4. Measurement of ALAAT2 aminotransferase activity with different substrates. Recombinant ALAAT2 was overexpressed in *E. coli* and activity was measured from crude extracts with different donor and acceptor substrates. Activites measured from a strain overexpressing an unrelated protein were substracted from those measured from ALAAT2 overexpressors. Shown are the means ±SE from three independent experiments. AGA, alanine:glyoxylate aminotransferase activity; AKA, alanine:ketoglutarate aminotransferase activity; GGA, glutamate:glyoxylate aminotransferase activity; GPA, glutamate:pyruvate aminotransferase activity.
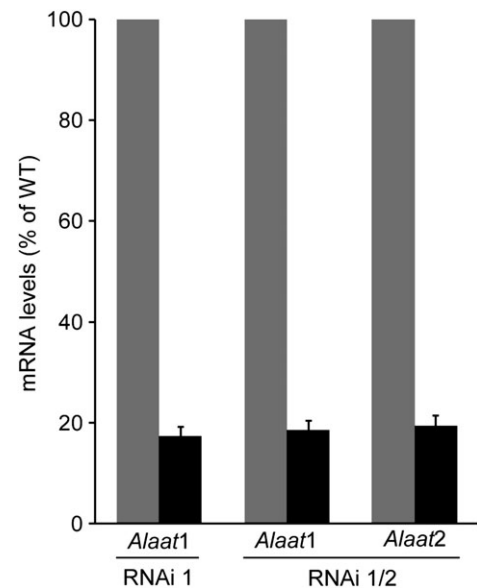

Fig. 5. Down-regulation of *Alaat*1 and *Alaat*2 expression by RNAi. Expression of *Alaat*1 and *Alaat*2 was measured in RNAi 1 and RNAi 1/2 lines (black bars) in comparison with wild-type expression (grey bars). Wild-type expression was set to 100%. Shown are the means ±SE from each 18 independent plants.

1 line, activities were slightly less reduced, but still significantly different from wild-type levels, indicating that ALAAT1 activity is suppressed in RNAi lines.

Both the RNAi 1 and the RNAi 1/2 line did not show any obvious phenotype under short-day growth conditions.
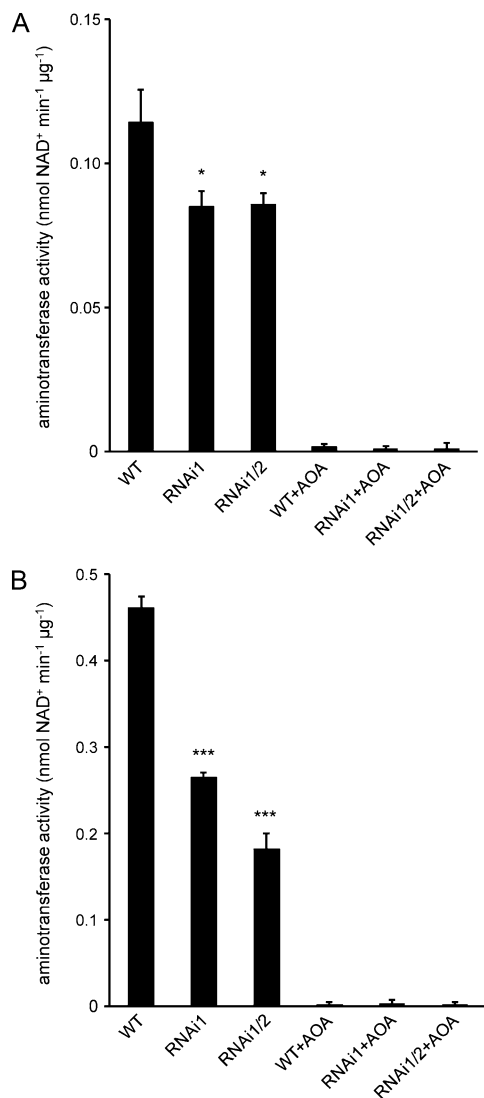
A

B

Fig. 6. Alanine aminotransferase activity in wild-type (WT), *Alaat*1 knock-down plants (RNAi 1), and *Alaat*1/*Alaat*2 double knock-down plants (RNAi 1/2). (A) Alanine:glyoxylate aminotransferase activity. (B) Alanine:ketoglutarate aminotransferase. AOA was used as an aminotransferase inhibitor. Shown are the means ±SE from three independent experiments. *$P < 0.05$; ***$P < 0.005$.

Because it was suspected that ALAATs were involved in photorespiration, metabolite profiles were determined from plants grown under normal CO_2 concentrations and from plants that were shifted to 100 ppm CO_2 for 24 h. Selected results are shown in Table 2, and a complete profile with 50 identified metabolites is available in Supplementary Table S1 at *JXB* online. Glycine levels increased in plants shifted to 100 ppm CO_2, indicating that flux through the photorespiratory pathway was enhanced, but no significant differences were observed between the genotypes under these conditions. Serine levels remained almost unchanged in wild types and RNAi lines. Induction of photorespiration at 100 ppm CO_2 strongly reduced glucose and fructose contents in leaves, whereas sucrose levels were only slightly affected by the low CO_2 stimulus. Again, no significant differences between wild-type plants and RNAi lines with reduced ALAAT expression

were observed. For the additionally tested metabolites (Supplementary Table S1), no differences were observed between the genotypes at 400 ppm CO_2. Only those differences were taken into consideration where both RNAi lines differed significantly from the wild type. At 100 ppm, only contents of arabinose and galactinol were increased in both RNAi lines compared with the wild type. Both substances do not have obvious links to mitochondrial amino acid metabolism. Overall, metabolite profiling did not reveal an obvious role in metabolism for ALAATs. However, the data also indicate that basal mitochondrial functions are not perturbed in RNAi lines.

Photosynthetic parameters of wild-type and RNAi lines at different CO_2 concentrations are shown in Table 3. Basic gas exchange parameters, such as apparent CO_2 assimilation (A) and intercellular CO_2 concentration (c_i), were affected by the low CO_2 treatment, but no differences between the genotypes were observed. The same pattern applied for photochemical quenching (qP) and non-photochemcial quenching (NPQ), as well as the actual quantum efficiency of photosystem II (ΦPSII). The maximum quantum efficiency of PSII (F_v/F_m) and stomatal conductance to CO_2 (g_s) were not affected by either the CO_2 treatment or RNAi suppression of *Alaat*1 and *Alaat*2 expression. However, when calculating the CO_2 compensation point by linear regression of A/c_i curves at low CO_2 concentrations, a significant reduction in both RNAi lines compared with the wild type was observed. This observation was further analysed by determining the post-illumination CO_2 burst (PIB) which is an estimate for the amount of CO_2 released from mitochondria during photorespiration in intact plants (Atkin *et al.*, 1998). Both RNAi 1 and RNAi 1/2 plants showed significant reductions in PIB. However, dark respiration rates (R_D) were unaffected, suggesting that differences in PIB are due to a reduction in photorespiratory flux.

In order to evaluate further the role of *Alaat*1 and *Alaat*2 in mitochondrial metabolism, $^{14}CO_2$ release from [^{14}C]glycolate in mitochondria isolated from wild-type and RNAi plants was compared (Fig. 7). Down-regulation of *Alaat*1 alone resulted in a reduction of CO_2 release to less than half the wild-type levels. This value was further reduced by simultaneous suppression of both *Alaat*1 and *Alaat*2 expression (Fig. 7A). In a complementary approach, ALAAT1 and/or GlcDH were transiently overexpressed by infiltration of *Agrobacterium* carrying the respective constructs into tobacco leaves. As a control, infiltration of *Agrobacterium* carrying a plasmid for overexpression of RFP was used. As shown in Fig. 7B, overexpression of ALAAT1 or GlcDH alone resulted in a comparable increase in CO_2 release of ~65%. The simultaneous overexpression of both proteins caused a 2.5-fold enhancement compared with the control.

The existence of a mitochondrial glycolate oxidation pathway might be a peculiarity of *Arabidopsis*. To test whether this pathway exists in other plants, glycolate conversion was measured in isolated mitochondria from the monocotyledoneous model plant rice (*O. sativa*). Recent characterization of the rice mitochondrial proteome indicated that rice mitochondria contain homologues of both At5g05680 and ALAAT1

Table 2. Relative amounts of selected metabolites at 400 ppm and 100 ppm CO_2

Substance	WT		RNAi 1		RNAi 1/2	
	400 ppm	100 ppm	400 ppm	100 ppm	400 ppm	100 ppm
Glycine	383.8±41.4	749.2±21.1	606.5±95.0	862.7±46.9	453.0±30.8	773.4±32.6
Serine	737.7 ±71.8	779.6±38.9	766.6 ±98.7	765.3±32.4	748.8±60.1	702.4±33.7
Glucose	514.9±107.3	177.3±34.5	640.6±117.8	241.1±23.7	442.3±49.7	227.5±21.3
Fructose	433.4±123.5	45.3±8.0	465.9±64.6	56.5±7.9	410.3±116.3	56.6±10.2
Sucrose	923.4±19.3	802.2±32.4	951.1±23.5	851.5±12.7	921.5±12.2	847.8±14.1

Shown are the relative amounts of metabolites identified by GC-MS from wild-type (WT) and RNAi plants grown at 400 ppm and 100 ppm CO_2 in arbitrary numbers.
Values are means ±SE of four biological replicates with a pool size of six plants per genotype and replicate.

Table 3. Gas exchange and chlorophyll fluorescence parameters of wild-type (WT) and RNAi plants

Parameter	WT		RNAi 1		RNAi 1/2	
	400 ppm	100 ppm	400 ppm	100 ppm	400 ppm	100 ppm
A (μmol m^{-2} s^{-1})	7.89±0.69	1.13±0.09	8.66±0.46	1.18±0.11	8.92±0.29	1.36±0.11
c_i (ppm CO_2)	311.93±8.35	86.72±1.14	315.25±6.24	88.54±0.6	312.56±5.42	85.69±1.43
g_s (μmol m^{-2} s^{-1})	0.18±0.01	0.17±0.02	0.20±0.02	0.21±0.02	0.20±0.02	0.19±0.02
qP	0.25±0.02	0.16±0.01	0.24±0.02	0.15±0.01	0.26±0.01	0.17±0.01
NPQ	1.93±0.09	1.98±0.10	1.84±0.08	1.99±0.07	1.97±0.05	2.07±0.05
F_v/F_m	0.79±0.004	0.79±0.004	0.79±0.003	0.79±0.003	0.80±0.002	0.80±0.002
ΦPSII	49.44±4.22	29.40±1.95	48.73±3.62	28.60±2.19	53.17±2.25	30.93±1.70
Γ (ppm CO_2)	63.88±1.09		59.29±0.90**		58.66±0.84**	
PIB (μmol m^{-2} s^{-1})	0.66±0.05		0.49±0.05*		0.44±0.03***	
R_D (μmol m^{-2} s^{-1})	1.03±0.15		1.03±0.06		1.11±0.03	

A, apparent CO_2 assimilation; c_i, intercellular CO_2 concentration; g_s, stomatal conductance; qP, photochemical quenching; NPQ, non-photochemical quenching; F_v/F_m, maximum quantum efficiency of photosystem ll; ΦPSII, actual quantum efficiency of photosystem ll; Γ, apparent CO_2 compensation point; PIB, post-illumination CO_2 burst; R_D, dark respiration.
Each data point represents the means ±SE of at least eight independent plants. For PIB and R_D, four independent plants were measured. All plants were 6–7 weeks old. *$P < 0.05$; **$P < 0.01$; ***$P < 0.005$.

from *Arabidopsis* (Os07g08950 and Os07g42600; Huang *et al.*, 2009). Figure 8A shows the formation of glyoxylate from glycolate in isolated mitochondria from rice. The observed activity is similar to what was described for *Arabidopsis* before (Niessen *et al.*, 2007). Glyoxylate formation could be suppressed by KCN that had been shown to inhibit GlcDH activity (Lord, 1972). However, no suppression was observed when AOA was added to the assay as aminotransferase activity is not required for glyoxylate formation from glycolate. In contrast, AOA was capable of suppressing CO_2 release from glycolate in isolated rice mitochondria (Fig. 8B), indicating that the further conversion of glyoxylate produced by the GlcDH reaction includes an aminotransferase step. The observed reduction was not due to a suppression of glycine decarboxylation by the amounts of AOA used in this assay. Thus, mitochondrial glycolate oxidation and transamination described in *Arabidopsis* is conserved in the monocot rice.

Discussion

Here, the function of two mitochondrial ALAATs in *Arabidopsis* was characterized. The enzymes were selected based on their homology to one out of three human ALAATs and to peroxisomal GGAT enzymes contributing to the major photorespiratory pathway (Igarashi *et al.*, 2003; Liepman and Olsen, 2003). RNAi lines against *Alaat*1 or both *Alaat*1 and *Alaat*2 show reduced accumulation of the respective mRNAs (Fig. 5) as well as a reduction by up to 70% in ALAAT activity assays (Fig. 6) from leaf extracts. This is in accordance with the previous characterization of an *Alaat*1 knock-out line that showed a similar reduction in leaf ALAAT activity (Miyashita *et al.*, 2007). However, aminotransferases often show broad substrate specificity *in vitro* and endogenous substrates are difficult to determine (Mehta *et al.*, 1993). Several lines of evidence suggest that the two characterized enzymes use glyoxylate and alanine as substrates *in vivo*: alanine enhances conversion of glycolate to CO_2 in isolated mitochondria (Niessen *et al.*, 2007) whereas the aminotransferase inhibitor AOA inhibits this reaction (Fig. 1). Mutation of the putative GlcDH (Niessen *et al.*, 2007) or down-regulation of ALAATs (Fig. 7) reduced this reaction, whereas overexpression of both proteins enhanced CO_2 release. These data indicate that GlcDH and ALAATs are necessary and sufficient for CO_2 release from labelled glycolate in isolated mitochondria. In intact leaves, down-regulation of ALAATs reduced the PIB (Table 3). This method is based on determining the difference between the maximum CO_2 release of a leaf when shifting the
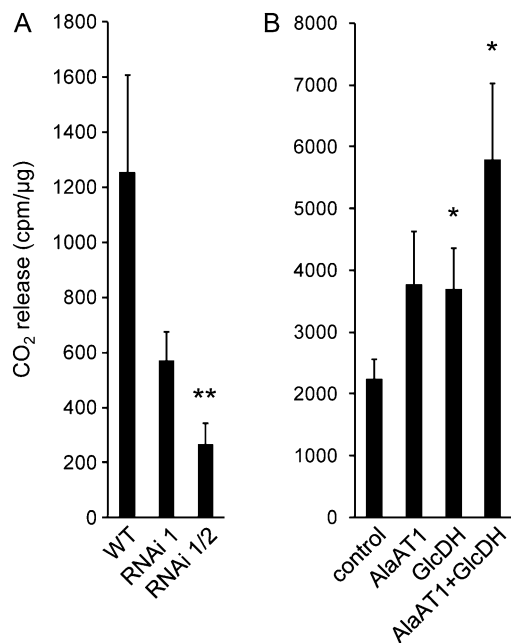
Fig. 7. Mitochondrial glycolate conversion in *Arabidopsis* RNAi lines and transiently overexpressing tobacco plants. Isolated mitochondria corresponding to 50 µg of protein were incubated with [^{14}C]glycolate. $^{14}CO_2$ released was captured in NaOH and determined by scintillation counting. (A) $^{14}CO_2$ release in mitochondria from wild-type (WT), *Alaat*1 knock-down plants (RNAi 1), and *Alaat*1/*Alaat*2 double knock-down plants (RNAi 1/2). (B) $^{14}CO_2$ release in transiently transformed tobacco plants overexpressing red fluorescent protein (control), AlaAT1, GlcDH, or both AlaAT1 and GlcDH (AlaAT1+GlcDH). Shown are the means ±SE from at least three independent experiments. cpm, counts per minute; *$P < 0.05$; **$P < 0.01$.

plant to darkness and the steady-state dark respiration (R_D) after the remaining photorespiratory glycine has been fully decarboxylated (Atkin *et al.*, 1998). As R_D remained unchanged, the most probable interpretation of the decrease in PIB is a reduction in photorespiratory CO_2 release. Sharkey (1988) argued that these measurements do not provide an accurate estimate of the photorespiratory flux as CO_2 assimilation might also occur shortly after darkening and respiration is variable during this time period. However, reproducible values for maximum and steady-state CO_2 release were observed under the present assay conditions. Thus, even if PIB measurements do not provide absolute numbers for photorespiratory flux, the relative reduction is indicative of changes in photorespiratory CO_2 release. Consistent with this observation, the CO_2 compensation point (Table 3), where photosynthetic CO_2 uptake matches respiratory and photorespiratory CO_2 release, is also reduced in RNAi 1 and RNAi 1/2 lines.

One reasonable explanation for the observed experimental data is that some of the glyoxylate produced in the photorespiratory pathway is not converted to glycine and thus not decarboxylated, but accumulates. The gas chromatography–tandem mass spectrometry (GC-MS) analyses were inappropriate for the unambiguous detection of gly-
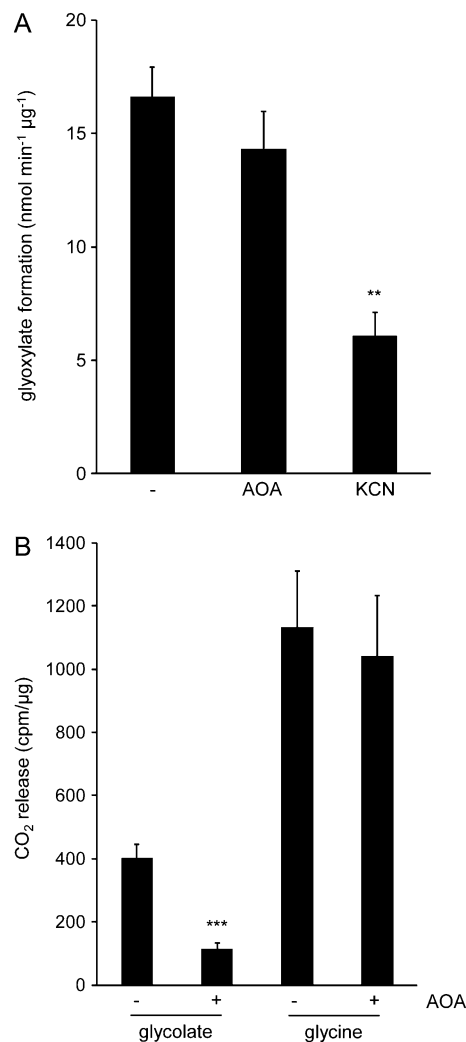

Fig. 8. Conservation of mitochondrial glycolate oxidation in rice. Glyoxylate formation was measured from isolated rice mitochondria. (A) GlcDH activity assay. Aminooxyacetate (AOA) or potassium cyanide (KCN) were added as inhibitors. (B) $^{14}CO_2$ release from isolated mitochondria with three different ^{14}C-labelled substrates. AOA was added as an inhibitor. Values for all ^{14}C-labelled substrates are corrected for the specific activity of each substrate. Shown are the means ±SE from at least three independent experiments. cpm, counts per minute; **$P < 0.01$; ***$P < 0.005$.

oxylate levels, but glycolate or glycine levels were not significantly changed (Table 2; Supplementary Table S1 at *JXB* online). Moreover, the RNAi lines did not show a growth phenotype—in contrast to most mutants in enzymes of the major photorespiratory pathway (Peterhansel *et al.*, 2010). These contradictory results might be explained by the different durations of the low CO_2 treatment. Plants were shifted to low CO_2 for a few minutes during gas exchange measurements, but for 24 h for the determination of metabolite levels. Thus, mitochondrial glycolate conversion might play a role under rapidly changing conditions, but not under steady-state conditions where the capacities of the major pathway are adjusted to the amounts of phosphoglycolate produced. Metabolic flux measurements instead of steady-state metabolite concentrations under different

conditions might reveal further insights into the contribution of ALAATs to glycine production.

A basal CO_2 release from glycolate was observed even in plants where the mitochondrial glycolate oxidation pathway was disrupted by down-regulation of ALAAT 1/2 (Fig. 7). This was not due to non-enzymatic decay of the labelled compound, because much lower levels of CO_2 release were observed in heat-inactivated extracts (data not shown). Other enzymes might partially compensate for reduced ALAAT abundance in RNAi lines. A mitochondrial γ-aminobutyrate (GABA) transaminase that can use glyoxylate as an amino group acceptor has recently been described and suggested to be involved in mitochondrial glycolate metabolism (Clark *et al.*, 2009). As GABA levels increase under stress, the amino donor might be available at high concentrations under photorespiratory conditions (Allan *et al.*, 2009). Alternatively, the remaining activity in the mutants might be caused by contamination with peroxisomes as peroxisomal glycolate oxidase and glyoxylate aminotransferase show much higher activities compared with the corresponding mitochondrial activities. However, the clear reduction in CO_2 release from glycolate in ALAAT RNAi lines (Fig. 7) indicates that these mitochondrial proteins are responsible for the bulk glycolate conversion in the mitochondrial preparations used here. It is also unlikely that the observed data were caused by an indirect effect of ALAAT 1/2 suppression on basal metabolism in RNAi lines as metabolite profiles and photosynthetic parameters were very similar for wild types and RNAi lines.

Glyoxylate produced in photorespiration is normally transaminated in peroxisomes (see Introduction). One function of ALAATs could be to convert excess glyoxylate that might diffuse from peroxisomes to mitochondria as suggested before for formate resulting from the decarboxylation of glyoxylate (Wingler *et al.*, 1999; Cousins *et al.*, 2008). Alternatively, a mitochondrial GlcDH might convert photorespiratory glycolate to glyoxylate and provide substrate for ALAATs. This scenario is consistent with the CO_2 release assays that use glycolate as a substrate (Figs 1, 7) and previous results showing that mitochondria contain a GlcDH that is involved in photorespiration (Niessen *et al.*, 2007). These data suggest that mitochondrial GlcDH and ALAATs are conserved from chlorophytes that use homologous enzymes for photorespiration (Nakamura *et al.*, 2005; Stabenau and Winkler, 2005). However, this is in contradiction to the very low turnover rates of the recombinant and purified putative GlcDH with glycolate as a substrate and the growth inhibition of knock-out lines on agar plates containing D-lactate, but not glycolate (Engqvist *et al.*, 2009). Similarly, ALAAT1 has been described before to contribute to the rapid conversion of alanine during the post-hypoxia recovery period in roots (Miyashita *et al.*, 2007). The nearest homologue to *Arabidopsis* ALAAT enzymes in *Medicago truncatula* has been shown to be induced in the embryo axis of young seedlings under hypoxia and to catalyse alanine synthesis instead of using alanine as an amino donor. However, the same enzyme catalyses glutamate synthesis from alanine and oxoglutarate under non-hypoxic conditions (Ricoult *et al.*, 2006). Thus, these enzymes might take over different functions in different tissues or under different conditions. Other isoforms of photorespiratory enzymes are also highly expressed in non-photosynthetic tissues such as roots (Foyer *et al.*, 2009) where they probably take over functions in pathways other than photorespiration. Thus, substrate availability dependent on the conditions instead of enzymatic specificity might regulate the function of photorespiratory enzymes as suggested before for the synthesis of secondary metabolites (Schwab, 2003) or the activities of glycosyltransferases (Bowles *et al.*, 2006).

Mitochondrial glycolate oxidation is just one of several alternative photorespiratory side pathways in higher plants. Beside peroxisomal glyoxylate decarboxylation mentioned above, there is also evidence that chloroplasts contain their own pathway for glycolate oxidation in addition to peroxisomes and mitochondria (Goyal and Tolbert, 1996; Kebeish *et al.*, 2007). Recently, it has been described that hydroxypyruvate can be reduced by cytoplasmic or chloroplastic isozymes instead of the peroxisomal enzyme (Timm *et al.*, 2008, 2011). All these alternative reactions might act as overflow valves for the major pathway to avoid accumulation of toxic intermediates. Alternatively, they can provide plants with metabolic flexibility. A major advantage of the mitochondrial pathway is the energy balance: glycolate oxidation can be linked to ATP synthesis instead of producing H_2O_2 in peroxisomes that has to be detoxified (Paul and Volcani, 1976; Stabenau and Winkler, 2005). This is probably important under low light conditions or in shaded leaves where energy supply is limiting growth (Gibon *et al.*, 2009). The data obtained from rice mitochondria suggest that glycolate dehydrogenase and glyoxylate aminotransferase activity have been conserved in both the dicot and monocot lineages (Fig. 8). Such evolutionary conservation supports the hypothesis that these activities provide plants with a selective advantage under natural conditions and constitute more than a remnant from green algae lacking leaf-type peroxisomes. Whether this selective advantage is based on function of these enzymes in glycolate metabolism or alternative acitvities remains to be shown.

Supplementary data

Supplementary data are available at *JXB* online.

Figure S1. Expression of putative RNAi targets and putative alanine aminotransferases.

Table S1. List of metabolites identified in wild-type and RNAi plants.

Acknowledgements

References

Allan WL, Clark SM, Hoover GJ, Shelp BJ. 2009. Role of plant glyoxylate reductases during stress: a hypothesis. *Biochemical Journal* **42,** 15–22.

Atkin OK, Evans JR, Siebke K. 1998. Relationship between the inhibition of leaf respiration by light and enhancement of leaf dark respiration following light treatment. *Australian Journal of Plant Physiology* **25,** 437–443.

Bari R, Kebeish R, Kalamajka R, Rademacher T, Peterhänsel C. 2004. A glycolate dehydrogenase in the mitochondria of Arabidopsis thaliana. *Journal of Experimental Botany* **55,** 623–630.

Bowles D, Lim EK, Poppenberger B, Vaistij FE. 2006. Glycosyltransferases of lipophilic small molecules. *Annual Review of Plant Biology* **57,** 567–597.

Carrie C, Kühn K, Murcha MW, Duncan O, Small ID, O'Toole N, Whelan J. 2009. Approaches to defining dual-targeted proteins in Arabidopsis. *The Plant Journal* **57,** 1128–1139.

Chomczynski P, Mackey K. 1995. Substitution of chloroform by bromo-chloropropane in the single-step method of RNA isolation. *Analytical Biochemistry* **225,** 163–164.

Clark SM, Di Leo R, Dhanoa PK, Van Cauwenberghe OR, Mullen RT, Shelp BJ. 2009. Biochemical characterization, mitochondrial localization, expression, and potential functions for an Arabidopsis γ-aminobutyrate transaminase that utilizes both pyruvate and glyoxylate. *Journal of Experimental Botany* **60,** 1743–1757.

Clough SJ, Bent AF. 1998. Floral dip: a simplified method for Agrobacterium-mediated transformation of Arabidopsis thaliana. *The Plant Journal* **16,** 735–743.

Cousins AB, Pracharoenwattana I, Zhou W, Smith SM, Badger MR. 2008. Peroxisomal malate dehydrogenase is not essential for photorespiration in Arabidopsis but its absence causes an increase in the stoichiometry of photorespiratory CO_2 release. *Plant Physiology* **148,** 786–795.

Emanuelsson O, Nielsen H, Brunak S, von Heijne G. 2000. Predicting subcellular localization of proteins based on their N-terminal amino acid sequence. *Journal of Molecular Biology* **300,** 1005–1016.

Engqvist M, Drincovich MF, Flugge U-I, Maurino VG. 2009. Two D-2-hydroxyacid dehydrogenases in Arabidopsis thaliana with catalytic capacities to participate in the last reactions of the methylglyoxal and β-oxidation pathways. *Journal of Biological Chemistry* **284,** 25026–25037.

Foyer CH, Bloom AJ, Queval G, Noctor G. 2009. Photorespiratory metabolism: genes, mutants, energetics, and redox signaling. *Annual Review of Plant Biology* **60,** 455–484.

Gibon Y, Pyl E-T, Sulpice R, Lunn JE, Höhne M, Günther M, Stitt M. 2009. Adjustment of growth, starch turnover, protein content and central metabolism to a decrease of the carbon supply when Arabidopsis is grown in very short photoperiods. *Plant, Cell and Environment* **32,** 859–874.

Goyal A, Tolbert NE. 1996. Association of glycolate oxidation with photosynthetic electron transport in plant and algal chloroplasts. *Proceedings of the National Academy of Sciences, USA* **93,** 3319–3324.

Heazlewood JL, Verboom RE, Tonti-Filippini J, Small I, Millar AH. 2007. SUBA: the Arabidopsis subcellular database. *Nucleic Acids Research* **35,** D213–D218.

Hruz T, Laule O, Szabo G, Wessendorp F, Bleuler S, Oertle L, Widmayer P, Gruissem W, Zimmermann P. 2008. Genevestigator v3: a reference expression database for the meta-analysis of transcriptomes. *Advances in Bioinformatics* **2008,** 420–747.

Huang S, Taylor NL, Narsai R, Eubel H, Whelan J, Millar AH. 2009. Experimental analysis of the rice mitochondrial proteome, its biogenesis, and heterogeneity. *Plant Physiology* **149,** 719–734.

Igarashi D, Miwa T, Seki M, Kobayashi M, Kato T, Tabata S, Shinozaki K, Ohsumi C. 2003. Identification of photorespiratory glutamate:glyoxylate aminotransferase (GGAT) gene in Arabidopsis. *The Plant Journal* **33,** 975–987.

Jach G, Binot E, Frings S, Luxa K, Schell J. 2001. Use of red fluorescent protein from Discosoma sp. (dsRED) as a reporter for plant gene expression. *The Plant Journal* **28,** 483–491.

Kebeish R, Niessen M, Thiruveedhi K, Bari R, Hirsch H-J, Rosenkranz R, Stäbler N, Schönfeld B, Kreuzaler F, Peterhänsel C. 2007. Chloroplastic photorespiratory bypass increases photosynthesis and biomass production in Arabidopsis thaliana. *Nature Biotechnol* **25,** 593–599.

Lee CP, Eubel H, O'Toole N, Millar AH. 2008. Heterogeneity of the mitochondrial proteome for photosynthetic and non-photosynthetic Arabidopsis metabolism. *Molecular and Cellular Proteomics* **7,** 1297–1316.

Liepman AH, Olsen LJ. 2001. Peroxisomal alanine:glyoxylate aminotransferase (AGT1) is a photorespiratory enzyme with multiple substrates in Arabidopsis thaliana. *The Plant Journal* **25,** 487–498.

Liepman AH, Olsen LJ. 2003. Alanine aminotransferase homologs catalyze the glutamate:glyoxylate aminotransferase reaction in peroxisomes of Arabidopsis. *Plant Physiology* **131,** 215–227.

Lisec J, Schauer N, Kopka J, Willmitzer L, Fernie AR. 2006. Gas chromatography mass spectrometry-based metabolite profiling in plants. *Nature Protocols* **1,** 387–396.

Lord JM. 1972. Glycolate oxidoreductase in *Escherichia coli*. *Biochimica et Biophysica Acta* **267,** 227–237.

Luedemann A, Strassburg K, Erban A, Kopka J. 2008. TagFinder for the quantitative analysis of gas chromatography and mass spectrometry (GC-MS)-based metabolite profiling experiments. *Bioinformatics* **24,** 732–737.

Maurino VG, Peterhansel C. 2010. Photorespiration: current status and approaches for metabolic engineering. *Current Opinion in Plant Biology* **13,** 249–256.

Mehta PK, Hale TI, Christen P. 1993. Aminotransferases: demonstration of homology and division into evolutionary subgroups. *European Journal of Biochemistry* **214,** 549–561.

Miyashita Y, Dolferus R, Ismond KP, Good AG. 2007. Alanine aminotransferase catalyses the breakdown of alanine after hypoxia in Arabidopsis thaliana. *The Plant Journal* **49,** 1108–1121.

Nakamura Y, Kanakagiri S, Van K, He W, Spalding M. 2005. Disruption of the glycolate dehydrogenase gene in the high-CO_2-requiring mutant HCR89 of Chlamydomonas reinhardtii. *Canadian Journal of Botany* **83,** 820–833.

Niessen M, Thiruveedhi K, Rosenkranz R, Kebeish R, Hirsch H-J, Kreuzaler F, Peterhansel C. 2007. Mitochondrial glycolate oxidation contributes to photorespiration in higher plants. *Journal of Experimental Botany* **58,** 2709–2715.

Paul JS, Volcani BE. 1976. A mitochondrial glycolate: cytochrome C reductase in Chlamydomonas reinhardii. *Planta* **129,** 59–61.

Peterhansel C, Horst I, Niessen M, Blume C, Kebeish R, Kürkcüoglu S, Kreuzaler F. 2010. *Photorespiration. The Arabidopsis book*. The American Society of Plant Biologists .

Rasmusson AG, Geisler DA, Moller IM. 2008. The multiplicity of dehydrogenases in the electron transport chain of plant mitochondria. *Mitochondrion* **8,** 47–60.

Raven JA. 2000. Land plant biochemistry. *Philosophical Transactions of the Royal Society B: Biological Sciences* **355,** 833–846.

Reumann S, Quan S, Aung K, *et al*. 2009. In-depth proteome analysis of Arabidopsis leaf peroxisomes combined with *in vivo* subcellular targeting verification indicates novel metabolic and regulatory functions of peroxisomes. *Plant Physiology* **150,** 125–143.

Ricoult C, Echeverria LO, Cliquet J-B, Limami AM. 2006. Characterization of alanine aminotransferase (AlaAT) multigene family and hypoxic response in young seedlings of the model legume Medicago truncatula. *Journal of Experimental Botany* **57,** 3079–3089.

Sarojini G, Oliver DJ. 1985. Inhibition of glycine oxidation by carboxymethoxylamine, methoxylamine, and acethydrazide. *Plant Physiology* **77,** 786–789.

Schwab W. 2003. Metabolome diversity: too few genes, too many metabolites? *Phytochemistry* **62,** 837–849.

Sharkey TD. 1988. Estimating the rate of photorespiration in leaves. *Physiologia Plantarum* **73,** 147–152.

Spalding MH. 2008. Microalgal carbon-dioxide-concentrating mechanisms: Chlamydomonas inorganic carbon transporters. *Journal of Experimental Botany* **59,** 1463–1473.

Sparkes IA, Runions J, Kearns A, Hawes C. 2006. Rapid, transient expression of fluorescent fusion proteins in tobacco plants and generation of stably transformed plants. *Nature Protocols* **1,** 2019–2025.

Stabenau H, Winkler U. 2005. Glycolate metabolism in green algae. *Physiologia Plantarum* **123,** 235–245.

Timm S, Florian A, Jahnke K, Nunes-Nesi A, Fernie AR, Bauwe H. 2011. The hydroxypyruvate-reducing system in Arabidopsis thaliana—multiple enzymes for the same end. *Plant Physiology* **155,** 694–705.

Timm S, Nunes-Nesi A, Parnik T, Morgenthal K, Wienkoop S, Keerberg O, Weckwerth W, Kleczkowski LA, Fernie AR, Bauwe H. 2008. A cytosolic pathway for the conversion of hydroxypyruvate to glycerate during photorespiration in Arabidopsis. *The Plant Cell* **20,** 2848–2859.

Wingler A, Lea PJ, Leegood RC. 1999. Photorespiratory metabolism of glyoxylate and formate in glycine-accumulating mutants of barley and Amaranthus edulis. *Planta* **207,** 518–526.